

RESEARCH ARTICLE

MATERIALS SCIENCE

Scalable fabrication of printed Zn//MnO₂ planar micro-batteries with high volumetric energy density and exceptional safety

Xiao Wang^{1,2}, *Shuanghao Zheng*^{1,2,3}, *Feng Zhou*¹, *Jieqiong Qin*^{1,2}, *Xiaoyu Shi*^{1,3,4}, *Sen Wang*^{1, 2}, *Chenglin Sun*¹, *Xinhe Bao*^{1,3,4}, *Zhong-Shuai Wu*^{1,*}

¹ Dalian National Laboratory for Clean Energy, Dalian Institute of Chemical Physics, Chinese Academy of Sciences, Dalian 116023, China

² University of Chinese Academy of Sciences, Beijing 100049, China

³ State Key Laboratory of Catalysis, Dalian Institute of Chemical Physics, Chinese Academy of Sciences, Dalian 116023, China

⁴ Department of Chemical Physics, University of Science and Technology of China, Hefei 230026, China

*E-mail: wuzs@dicp.ac.cn

ABSTRACT

The rapid development of printed and microscale electronics imminently requires their compatible micro-batteries (MBs) with high performance, applicable scalability, and exceptional safety, but facing great challenges from the ever-reported stacked geometry. Herein, the first printed planar prototype of aqueous-based, high-safe Zn//MnO₂ MBs, with outstanding performance, aesthetic diversity, flexibility and modularization, is demonstrated, based on interdigital patterns of Zn ink as anode and MnO₂ ink as cathode, with high-conducting graphene ink as metal-free current collector, fabricated by industrially scalable screen-printing technique. The planar separator-free Zn//MnO₂ MBs, tested in neutral aqueous electrolyte, deliver high volumetric capacity of 19.3 mAh/cm³ (corresponding to 393 mAh/g) at 7.5 mA/cm³, and notable volumetric energy density of 17.3 mWh/cm³, outperforming lithium thin-film batteries (≤ 10 mWh/cm³). Furthermore, our Zn//MnO₂ MBs present long-term cyclability having high capacity retention of 83.9% after 1300 times at 5 C, which is superior to stacked Zn//MnO₂ batteries reported. Also, Zn//MnO₂ planar MBs exhibit exceptional flexibility without observable capacity decay under serious deformation, and remarkably serial and parallel integration of constructing bipolar cells with high voltage and capacity output. Therefore, low-cost, environmentally benign Zn//MnO₂ MBs with in-plane geometry possess huge potential as high-energy, safe, scalable and flexible microscale power sources for direction integration with printed electronics.

Keywords: low cost, printed, planar, Zn//MnO₂ micro-batteries, metal-free current collectors

INTRODUCTION

The emerging smart printed electronics with the integrated features of exceptional flexibility, thinness, lightweight, and miniaturization have significantly inspired the relentless pursuit of low-cost, safe and environmentally benign printed microscale energy storage devices with high performance [1-5]. Lithium thin-film micro-batteries (MBs) with energy density of 10 mWh/cm^3 are the most popular microscale power sources for various microsystems. However, most reported MBs are usually constructed in a nonplanar stacked geometry, resulting in bulky volume, limited flexibility, and inconvenient serial and parallel connection via metal interconnects and current collectors. Also, such MBs are generally fabricated by the complicated manufacture processes, e.g., photolithographic technique, and present unsatisfactory safety issue with flammable organic electrolytes. To overcome this, developing aqueous based printed MBs with a separator-free planar geometry is acknowledged as a highly competitive class of microscale power sources due to the intrinsic nonflammability, high ionic conductivity of aqueous electrolytes [5-6], and great advances of planar device geometry with extremely short ion diffusion pathway [7-8]. It is noteworthy that the printed planar MBs are highly favorable for direct integration of printed electronics on a single substrate, simultaneously combining the characteristics of outstanding flexibility, designable shapes, adjustable sizes, and space-saving connections.

So far, various printing techniques have been developed for fabricating the traditional stacked batteries [9-11], such as lithium ion batteries by 3D printing [12], Zn-Ag batteries by inkjet printing [13], Zn-air batteries by screen printing [14]. Also, great progresses have been made for planar lithium thin-film MBs [15], lithium ion MBs [16], Zn//Ag₂O [3], Zn//LiMn₂O₄ [17], Zn//LiFePO₄ [17], 3D MBs [18-20], and

micro-supercapacitors [21-24] through the development of various micro-fabrication techniques, such as photolithography [25], electrodeposition [26], spraying [9,27], laser scribing [28], mask-assisted filtration [16], inkjet printing [10], roll-to-roll printing [29], and 3D printing [11-12]. In particular, screen printing can effectively control the precise pattern design with adjustable rheology of the inks, and is very promising for large-scale application [30]. Besides, screen printing is considerably recognized as a cost-effective, easy-processing, and mass-production methodology for the fast construction of MBs, having a precise control over the performance, flexibility, and integration with printed microelectronics. To address the cost effectiveness and safety issues, aqueous rechargeable Zn//MnO₂ batteries, characterized by high abundance, low cost, nontoxicity and safety of both Zn and MnO₂, as well as high output voltage of 0.9~1.8 V in aqueous electrolyte and large capacity of 820 mAh/g [31-33], are rising as one of the most compelling candidates [34-37]. Nevertheless, low cost and scalable fabrication of aqueous based planar Zn//MnO₂ MBs with multiple innovative form factors of high performance, flexibility, and integration still remains challenging.

Herein we reported a cost-effective and industrially applicable screen printing strategy for fast and scalable production of rechargeable planar Zn//MnO₂ MBs, featured with high performance, superior flexibility, scalable applicability, and high safety. The planar Zn//MnO₂ MBs, free of separators, were directly manufactured by directly printing the zinc ink as the anode (thickness of 6.4 μm) and γ-MnO₂ ink as the cathode (thickness of 9.8 μm), high-quality graphene ink as metal-free current collectors, working in environmentally benign neutral aqueous electrolytes of 2 M ZnSO₄ and 0.5 M MnSO₄. Benefiting from the suitable rheological properties of the inks and high electrical conductivity of microelectrodes (463 S/m for zinc anode, and 339 S/m for MnO₂ cathode), the as-fabricated Zn//MnO₂ MBs showed outstanding

volumetric capacity of 19.3 mAh/cm³ at 7.5 mA/cm³ (393 mAh/g at 154 mA/g), high energy density of 17.4 mWh/cm³, long-term cycling stability (~83.9% after 1300 at 5 C), designable shape, extraordinary flexibility, outstanding serial and parallel modularization for boosting the capacity and voltage output. Therefore, taking such very impressive performance into account, our Zn//MnO₂ MBs fabricated with screen-printing technology could potentially meet the stringent requirements of high performance, environmental friendliness, low cost, easy scalability, and high safety for printed electronics [38].

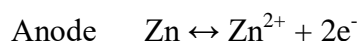
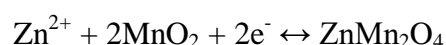
RESULTS AND DISCUSSION

The screen-printing fabrication of the interdigital planar Zn//MnO₂ MBs is schematically illustrated at Fig 1a-h. Firstly, highly stable and conductive graphene ink with appropriate rheological properties was printed on the substrates, e.g., flexible polyethylene terephthalate (PET), cloth, A4 paper, and even rigid glass (Figs 1 i-k), through stencil-printed process to form the interdigital planar patterns as metal-free current collectors, with a typical thickness of 1.4 μm, and exceptional electrical conductivity of 2.3×10^4 S/m (Fig. S1a, Supporting Information). Secondly, the anodic four fingers of asymmetric interdigital microelectrodes were deposited by extruding Zn based ink (33.3 wt% Zn microparticles) (Fig. 2a, Fig. S2a and S3a-b, Supporting Information) through the screen on one side of four graphene current collectors. Thirdly, the cathodic four fingers were manufactured by screen-printing γ -MnO₂ based ink (18.8 wt% MnO₂ nanoparticles) (Fig. 2b, Fig. S2b, S3c-d, and S4, Supporting Information) on the other side of four graphene-based current collectors. Notably, all inks possessed typical rheological behavior, showing the viscosity decreases with increasing shear rate keeping below 1 Pa·s from 10 to 8000 s⁻¹ (Fig. S5a-c, Supporting Information), which is highly important for precisely patterning

microelectrodes [38-39]. The screen-printed Zn based anode and MnO₂ based cathode (SEM, Fig. S6, Supporting Information), with a typical thickness of 6.4 and 9.8 μm (Fig. 2c-f), exhibited high electrical conductivity of ~320 and ~450 S/m (Fig. S1b-c, Supporting Information), respectively. It is noted that the as-fabricated planar Zn//MnO₂ MBs, with free of both separator and metal current collectors, exhibited extremely short ion diffusion distances [40-43], and robust flexibility without film fracture and delamination from the substrate under various bending states (Fig. 2g-m) [8]. Furthermore, our screen printing technique is highly simple, effective and scalable for low-cost scalable production of flexible and seamlessly integrated Zn//MnO₂ MBs with designable shapes and complex planar geometries, such as individual (Fig. 2g, j) and multiple parallel interdigital MBs via connection in series and in parallel (Fig. 2i, k), our institute logo MBs (Fig. 2h), tandem concentric circular (Fig. 2l) and linear MBs (Fig. 2m) not required of conventional metal based interconnectors. Finally, after adding the aqueous electrolyte (2 M ZnSO₄ and 0.5 M MnSO₄) onto the projected area of microelectrodes and packaging, the aqueous based planar Zn//MnO₂-MBs were obtained.

To demonstrate the outstanding electrochemical performance, we first measured galvanostatic charge and discharge (GCD) profiles of printed Zn//MnO₂ MBs at different current densities of 0.5 to 5 C (1 C= 308 mA/g, or 15 mA/cm³) between 0.9 and 1.8 V, using a neutral aqueous electrolyte containing 2 M ZnSO₄ and 0.5 M MnSO₄. It is pointed out that the presence of MnSO₄ can significantly prevent the dissolution of MnO₂, and improve the cyclability of Zn//MnO₂ MBs [43]. As expected, the addition of 0.5 M MnSO₄ into electrolyte indeed result in the impressively enhanced performance of Zn//MnO₂ MBs (Fig. S7a-b, Supporting Information) [43]. Apparently, our Zn//MnO₂ MBs displayed the similar discharge

voltage plateau at ~1.3 V observed at different current densities (Fig. 3a), originating from the intercalation mechanism in Zn//MnO₂ MBs. Specifically, the insertion and extraction process of both H⁺ and Zn²⁺ in the cathode are formulated as follows [44],



Regardless of the increased rates, it is observed that the polarization did not virtually increase at high discharge rates. Importantly, our MBs presented exceptionally high capacity at the different rates. It was revealed that the discharge capacity varies from 18.4 (5th cycle), 14.2 (15th cycle), 9.8 (25th cycle) to 7.7 (35th cycle) mAh/cm³ with increasing rates from 0.5, 1, 3 to 5 C, respectively (Figure 3b). Notably, the capacity thus readily returned back to 9.6 (45th cycle), 13.6 (55th cycle) and 19.3 (65th cycle) mAh/cm³ when the rates reversely back to 3, 1, and 0.5 C, respectively (Figure 3b).

The long-term cycling stability of Zn//MnO₂ MBs is one of the most important performance metrics for actual applications. Through the elaborated screening of cathodic MnO₂ and anodic zinc powder, selection of aqueous electrolytes (ZnSO₄ + MnSO₄), processing of highly stable and conducting inks, and usage of metal-free graphene current collectors, together with advanced planar geometry with shorter ion diffusion pathway and free of separator, and sophisticated screen-printing technique, synergistically working together, the resulting Zn//MnO₂ MBs showed remarkably satisfactory cycling performance (Fig. 3c-d, g). It is disclosed that, the planar Zn//MnO₂ MBs displayed impressive capacity of 15 mAh/cm³ over 100 cycles at a low current density of 1 C. In a sharp contrast, the stacked Zn//MnO₂ MBs based on sandwich-like Zn foil and MnO₂ electrode with a thickness of ~200 μm, prepared by

conventional blade coating (MnO_2 : acetylene black: polyvinylidene fluoride = 8:1:1), only showed about 4 mAh/cm^3 after 100 cycles at 1 C (Fig. 3d), which definitely identify the superior performance of the planar Zn//MnO_2 MBs. Importantly, the defined discharge voltage platform of GCD profiles was still well maintained (Fig. 3e), further demonstrative of outstanding structure stability of microelectrodes. What's more, the GCD profiles show that the capacity of planar MBs (15 mAh/cm^3) is much higher than the stacked MBs (4 mAh/cm^3). Electrochemical impedance spectroscopy (EIS) revealed that the slope of planar Zn//MnO_2 MBs is much higher than the stacked cell at the low frequency (Fig. 3f, Fig. S8), indicative of the faster ion diffusion in thinner thickness of microelectrodes of the planar MBs. Furthermore, our Zn//MnO_2 MBs displayed exceptionally long-term cycling stability, with a capacity retention of 83.9% even at a high rate of 5 C after 1300 cycles (Fig. 3g), outperforming the most reported Zn//MnO_2 batteries, such as $\text{Zn//}\beta\text{-MnO}_2$ (75% retention after 200 cycles) [31], Zn//MnO_2 @poly(3,4-ethylenedioxythiophene) (83.7% retention after 300 cycles) [34], yarn Zn//MnO_2 (98.5% retention after 500 cycles) [44], Zn//MnO_2 (81.5% retention after 1000 cycles) [27]. The capacity decay was mainly attributed to the slow dissolution and disruption of the MnO_2 cathode, the volume changes of microelectrodes owing to the big size of Zn^{2+} insertion/extraction, and the concomitant stresses on account of the irreversible side reaction [45]. And the capacity fluctuation of Zn//MnO_2 MBs was mainly caused by the slow and non-uniform permeation of aqueous electrolyte into the electrodes during the cycling process. Several factors working together were contributed to the outstanding electrochemical performance. First, metal-free graphene current collectors can significantly enhance the electrical conductivity of microelectrodes, and remarkably improve the rate capability of Zn//MnO_2 MBs. Secondly, compared with $\alpha\text{-MnO}_2$

[46], the cathode of γ -MnO₂ with the mix tunnels of (1×1) and (1×2), is favorable for the Zn²⁺ ions intercalation /deintercalation in Zn//MnO₂ MBs, and also highly active to proton cation, following the so-called two-step pathways in a mild electrolyte. Thirdly, the aqueous electrolyte containing the Zn²⁺ with a Mn²⁺ additive has high ionic conductivity of >1.0 S/cm, three orders of magnitude higher than organic electrolytes (10⁻³ S/cm) [47-48], thereby greatly hindering the pulverization and dissolution of MnO₂ and effectively improving the cyclability [49]. Last but not least, the polymer-assisted stable and conductive inks could substantially prevent the enormous volume change and the concomitant huge stress, thus contributing to the superior cyclability. As a result, the specific capacity and long-term cyclability of our Zn//MnO₂ MBs are much better than those reported Zn//MnO₂ batteries (Table S1 and Table S2).

To deeply understand the charge storage mechanism of Zn//MnO₂ MBs, we further examined the cyclic voltammetry (CV) curves tested at different scan rates (Fig. 4a). It is evident that the two pair redox peaks (1.6 vs. 1.35 V, and 1.52 vs. 1.22 V) of the CV curves became gradually broad with increasing scan rate, but their shapes kept almost consistent (Fig. 4a). To obtain the insight into the intrinsic mechanism of Zn//MnO₂ MBs, we further analyze the CV curves using the classic kinetics equations [50-51], $i = a v^b$ (or $\log i = \log a + b \log v$), where the current i obeys a power rule relationship with the scan rate v . Both a and b are the adjustable parameters. The value $b=0.5$ indicates a diffusion-controlled insertion process, while the b value of 1.0 represents a surface capacitive process. In term of this regulation, it is calculated that, for our Zn//MnO₂ MBs, the b values of four peaks are 0.875 (peak 1), 0.987 (peak 2), respectively (Fig. 4b), indicating that the electrochemical kinetics of Zn//MnO₂ MBs mainly involved the surface capacitive process, accompanied with

the diffusion-controlled intercalation process to some extent, contributing to the superior performance [1].

To meet the demands of future flexible and integrated microelectronics, developing flexible and integrated Zn//MnO₂ MBs is urgently required. To highlight this feature, we examined CV curves of Zn//MnO₂ MBs under varying bending angles from 0 to 180° at a scan rate of 1 mV/s (Fig. 5a). Apparently, it is confirmed that all the CV curves with typical battery behavior are well overlapped (Fig. 5b), along with extraordinary capacity retention of almost 100% even bended at 180 ° (Fig. 5c), suggestive of highly stable flexibility. It is attributed to the advance of separator-free planar geometry of Zn//MnO₂ MBs built on one substrate, which can greatly enhance the intimate contact between the microelectrodes and flexible PET substrate, without involving the multiple interfacial delamination of stacked MBs [17].

Furthermore, the integrated Zn//MnO₂ MBs were constructed via connection of multiple cells in series and in parallel (Fig. 5d), free of metal-based interconnects. It's worth noting that, from the GCD profiles, Zn//MnO₂ MBs connected in series displayed the analogical electrochemical properties, and simultaneously a stepwise increase of output voltage from 1.3 V for single cell to 2.6 V for two cells and 3.9 V for three cells (Fig. 5e), suggestive of exceptional performance uniformity. Moreover, in a parallel fashion, the volumetric capacity of the integrated Zn//MnO₂ MBs connected from 1 to 3 cells increased progressively, while the output voltage was almost kept unchanged (Fig. 5f). Notably, a tandem pack of two serially-connected Zn//MnO₂ MBs can readily power a light-emitting diodes (LED) for a significant long time under the flexible state, and lighted up a display screen of our institute "DICP" logo, manifesting enormous potential of our integrated Zn//MnO₂ MBs (Fig. 5g-h).

The volumetric energy density and power density are also the important performance metrics to evaluate microscale energy storage devices, thereby the Ragone plot was shown to compare our planar Zn//MnO₂ MBs with other miniaturized energy-storage devices (Fig. 5i). Encouragingly, our printed Zn//MnO₂ MBs could output maximum volumetric energy density of 17.3 mWh/cm³ at a power density of 150 mW/cm³. This energy density is much higher than the commercially available supercapacitors (SC: 1 mWh/cm³), Zn-ion microsupercapacitors (Zn-MS: 11.81 mWh/cm³) [2], and lithium thin-film battery (10 mWh/cm³) [52], ZnO//NiO (11 mWh cm⁻³) [53], NiO//Fe₃O₄ (1.83 mWh/cm³) [54]. What's more, the power density of Zn//MnO₂ MBs is 150 mW/cm³, three orders of magnitude higher than lithium thin-film battery (0.08 mW/cm³). Therefore, our printed Zn//MnO₂ MBs not only manifest the merits of the green, low-cost, scalable, and safe characteristics, but also possess high volumetric energy and power densities, endowing them numerous potential applications in miniaturized and printed electronics.

CONCLUSIONS

In summary, we have demonstrated the cost-effective and scalable fabrication of the rechargeable printed Zn//MnO₂ planar MBs, with intriguing features of scalability, environmentally benign, highly safety and metal-free current collectors, possessing high volumetric energy density, excellent rate capability and long-life cycling durability. Significantly, our printed Zn//MnO₂ MBs could be designed with various planar configurations, simultaneously representing designable artistic shapes, impressive flexibility, and remarkable modularization of building bipolar cells with high voltage and capacity output. More importantly, taking into the full considerations of low-cost and safe Zn, earth-abundant MnO₂, environmentally benign neutral aqueous electrolyte, and inexpensive screen-printing technology, our strategy of

constructing printed Zn//MnO₂ MBs hold great potential as next-generation microscale power sources in various wearable, flexible, miniaturized and printed electronics [18].

METHODS

Preparation of Zn Ink and MnO₂ Ink

Polyurethane resin (99%, Henan DaKen Chemical CO., Ltd.) was added into the dispersant of aromatic solvents (S150, 98%, Pengchen new material technology Co., Ltd.) and ethylene glycol diglycidyl ether (99%, Hangzhou Dayangchem Co., Ltd.). To fully dissolve the resin, the mixture was heated to 80 °C for 2 h. Subsequently, graphene (Nanjing XFNANO Materials Tech Co., Ltd), superfine graphite (Wuxi Hengtai metal material Co., Ltd.), carbon black (90%, Zhengzhou Blue Ribbon Industry Co., Ltd.) and MnO₂ powder (99.9%, Beijing DK nano technology Co. Ltd.) were put into the above resin solution with an intense stirring of 1500 r/min for 30 min. After the resultant precursor was subjected to be repeatedly grinded onto three-roll grinder, the MnO₂ ink was achieved. The mass proportion of polyurethane resin: graphene: superfine graphite: carbon black: MnO₂ powder is 3: 1: 1: 3: 2. The graphene conductive ink was prepared using the same reagent and procedure with graphene nanosheets (lateral size of 5~10 μm, 3~6 layers, Fig.S9), except no addition of MnO₂. The Zn ink was made by uniformly mixing the as-prepared conductive ink and zinc powder (6-9 μm, 97.5%, Alfa aesar) with the weight ratio of 2:1, when it was used.

Fabrication of Zn//MnO₂ MBs

Firstly, the highly conductive graphene ink was first printed on the PET, A4 paper, glass, or cloth substrates to form graphene-based current collectors, dried at 80 °C in vacuum box for 20 minutes until it was totally dried. Secondly, Zn based ink via the same approach was overlapped as anode on one side of graphene-based current collectors, while MnO₂ based ink was subsequently deposited as cathode on the other side of graphene-based current collectors. Then, the screen-printed asymmetric microelectrodes of Zn//MnO₂ MBs were dried at 80 °C for 12 h. Afterwards, the neutral aqueous electrolyte of 2 M ZnSO₄ and 0.5 M MnSO₄ was slowly dropped onto the project area of the microelectrodes and packaged with Kapton tape. Finally, the aqueous based printed Zn//MnO₂-MBs were obtained. Note that the interdigital customized screen has eight fingers, with length of 12 mm, width of 1 mm and interspace of 1 mm (Fig. S10).

Materials Characterization

The morphology, structure and composition of the active materials, graphene, the inks, and microelectrodes were analyzed using field-emission SEM (JSM-7800F), HRTEM (JEM-2100), XRD (X`pert Pro)(5° - 90°), four-point probe equipment (RTS-9), alpha step D-600, and thermogravimetric analysis (TGA, STA 449 F3)(measured at air atmosphere, 10°/min from 25 °C to 1000 °C).

Electrochemical Measurement

The CV curves obtained at varying scan rates of 0.1~0.4 mV/s and EIS tested from 100 kHz to 0.01Hz with an AC amplitude of 5 mV were conducted by an electrochemical workstation (CHI 760E), and the GCD profiles were measured by LAND CT2001A battery tester at the voltage of between 0.9 and 1.8 V at current densities from 0.5 to 5 C.

SUPPLEMENTARY DATA

Supplementary data are available at *NSR* online

FUNDING

This work was supported by the National Natural Science Foundation of China (51572259, 51872283 and 21805273), National Key R&D Program of China (2016YFB0100100 and 2016YFA0200200), LiaoNing Revitalization Talents Program (XLYC1807153), Natural Science Foundation of Liaoning Province (20180510038), Dalian Institute of Chemical Physics (DICP) (DICP ZZBS201708 and DICP ZZBS201802), Dalian National Laboratory For Clean Energy (DNL), Chinese Academy of Sciences (CAS), DICP & Qingdao Institute of BioEnergy and Bioprocess Technology (QIBEBT) (DICP&QIBEBT UN201702), DNL Cooperation Fund, CAS (DNL180310, DNL180308), Exploratory Research Program of Shaanxi Yanchang Petroleum (Group) CO., LTD & DICP.

REFERENCES

1. Chao, D. L., Zhu, C., and Song, M., *et.al.* A high-rate and stable quasi-solid-state zinc-ion battery with novel 2D layered zinc orthovanadate array. *Adv. Mater.* 2018; **30**: 1803181.
2. Sun, G. Q., Yang, H. S., and Zhang, G. F., *et.al.* A capacity recoverable zinc-ion micro-supercapacitor. *Energ. Environ. Sci.* 2018; **11**: 3367-74.
3. Kumar, R., Shin, J., and Yin, L., *et.al.* All-printed, stretchable Zn-Ag₂O rechargeable battery via hyperelastic binder for self-powering wearable electronics. *Adv. Energy Mater.* 2017; **7**: 1602096.
4. Choi, K.-H., Yoo, J., and Lee, C. K., *et.al.* All-inkjet-printed, solid-state flexible supercapacitors on paper. *Energ. Environ. Sci.* 2016; **9**: 2812-21.
5. Hondred, J. A., Stromberg, L. R., and Mosher, C. L., *et.al.* High-resolution graphene films for electrochemical sensing via inkjet maskless lithography. *ACS Nano* 2017; **11**: 9836-45.
6. Pan, H., Shao, Y., and Yan, P., *et.al.* Reversible aqueous zinc/manganese oxide energy storage from conversion reactions. *Nat. Energy* 2016; **1**: 16039.
7. Wu, Z. S., Parvez, K., and Feng, X. L., *et.al.* Graphene-based in-plane micro-supercapacitors with high power and energy densities. *Nat. Commun.* 2013; **4**: 2487.

8. Wu, Z. S., Feng, X. L. and Cheng, H. M. Recent advances in graphene-based planar micro-supercapacitors for on-chip energy storage. *Natl. Sci. Rev.* 2014; **1**: 277-92.
9. Singh, N., Galande, C., and Miranda, A., *et.al.* Paintable battery. *Sci. Rep.* 2012; **2**: 5.
10. Deiner, L. J. Reitz, T. L. Inkjet and aerosol jet printing of electrochemical devices for energy conversion and storage. *Adv. Energy Mater.* 2017; **19**: 1600878.
11. McOwen, D. W., Xu, S. M., and Gong, Y. H., *et.al.* 3D-printing electrolytes for solid-state batteries. *Adv. Mater.* 2018; **30**: 1707132.
12. Sun, K., Wei, T. S., and Ahn, B. Y., *et.al.* 3D printing of interdigitated Li-ion microbattery architectures. *Adv. Mater.* 2013; **25**: 4539-43.
13. Ho, C. C., Murata, K., Steingart, D. A., *et.al.* A super inkjet printed zinc–silver 3D microbattery. *J. Micromech. Microeng.* 2009; **19**: 094013.
14. Hilder, M.; Winther-Jensen, B., and Clark, N. B. Paper-based, printed zinc–air battery. *J. Power Sources* 2009; **194**: 1135–41.
15. Hu, L. B., Wu, H., and La Mantia, F., *et.al.* Thin, flexible secondary Li-ion paper batteries. *ACS Nano* 2010; **4**: 5843-48.
16. Zheng, S., Wu, Z.-S., and Zhou, F., *et.al.* All-solid-state planar integrated lithium ion micro-batteries with extraordinary flexibility and high-temperature performance. *Nano Energy* 2018; **51**: 613-20.

17. Zhao, J. W., Sonigara, K. K., and Li, J. J., *et.al.* A smart flexible zinc battery with cooling recovery ability. *Angew. Chem. Int. Ed.* 2017; **56**: 7871-75.
18. Wei, T. S., Ahn, B. Y., and Grotto, J., *et.al.* 3D printing of customized Li-ion batteries with thick electrodes. *Adv. Mater.* 2018; **30**: 1703027.
19. Oudenhoven, J. F. M., Baggetto, L. Notten, P. H. L. All-solid-state lithium-ion microbatteries: A review of various three-dimensional concepts. *Adv. Energy Mater.* 2011; **1**: 10-33.
20. Janoschka, T., Hager, M. D. Schubert, U. S. Powering up the future: Radical polymers for battery applications. *Adv. Mater.* 2012; **24**: 6397-409.
21. Wang, S., Wu, Z. S., and Zheng, S., *et.al.* Scalable fabrication of photochemically reduced graphene-based monolithic micro-supercapacitors with superior energy and power densities. *ACS Nano* 2017; **11**: 4283-91.
22. Xiao, H., Wu, Z.-S., and Zhou, F., *et.al.* Stretchable tandem micro-supercapacitors with high voltage output and exceptional mechanical robustness. *Energy Storage Mater.* 2018; **13**: 233-40.
23. Zheng, S., Ma, J., and Wu, Z.-S., *et.al.* All-solid-state flexible planar lithium ion micro-capacitors. *Energ. Environ. Sci.* 2018; **11**: 2001-09.
24. Zhou, F., Huang, H., and Xiao, C., *et.al.* Electrochemically scalable production of fluorine-modified graphene for flexible and high-energy ionogel-based microsupercapacitors. *J. Am. Chem. Soc.* 2018; **140**: 8198-205.

25. Wu, Z. S., Parvez, K., and Feng, X. L., *et.al.* Photolithographic fabrication of high-performance all-solid-state graphene-based planar micro-supercapacitors with different interdigital fingers. *J. Mater. Chem. A* 2014; **2**: 8288-93.
26. Lai, W. H., Wang, Y., Lei, and Z. W., *et.al.* High performance, environmentally benign and integratable Zn//MnO₂ microbatteries. *J. Mater. Chem. A* 2018; **6**: 3933-40.
27. Shi, X. Y., Wu, Z. S., and Qin, J. Q., *et.al.* Graphene-based linear tandem micro-supercapacitors with metal-free current collectors and high-voltage output. *Adv. Mater.* 2017; **29**: 1703034.
28. Xie, B. H., Wang, Y., Lai, and W. H., *et.al.* Laser-processed graphene based micro-supercapacitors for ultrathin, rollable, compact and designable energy storage components. *Nano Energy* 2016; **26**: 276-85.
29. Choi, K. H., Ahn, D. B. Lee, S. Y. Current status and challenges in printed batteries: Toward form factor-free, monolithic integrated power sources. *ACS Energy Lett.* 2018; **3**: 220-36.
30. Choi, K. H., Ahn, D. B. Lee, S. Y. Current status and challenges in printed batteries: Toward form factor-free, monolithic integrated power sources. *ACS Energy Lett.* 2018; **3**: 220-36.
31. Islam, S., Alfaruqi, M. H., and Mathew, V., *et.al.* Facile synthesis and the exploration of the zinc storage mechanism of β -MnO₂ nanorods with exposed

- (101) planes as a novel cathode material for high performance eco-friendly zinc-ion batteries. *J. Mater. Chem. A* 2017; **5**: 23299-309.
32. Huang, J., Wang, Z., and Hou, M., *et.al.* Polyaniline-intercalated manganese dioxide nanolayers as a high-performance cathode material for an aqueous zinc-ion battery. *Nat. Commun.* 2018; **9**: 2906.
33. Wang, Z., Ruan, Z., and Liu, Z., *et.al.* A flexible rechargeable zinc-ion wire-shaped battery with shape memory function. *J. Mater. Chem. A* 2018; **6**: 8549-57.
34. Zeng, Y. X., Zhang, X. Y., and Meng, Y., *et.al.* Achieving ultrahigh energy density and long durability in a flexible rechargeable quasi-solid-state Zn-MnO₂ battery. *Adv. Mater.* 2017; **29**: 1700274.
35. Zhang, N., Cheng, F. Y., and Liu, Y. C., *et.al.* Cation-deficient spinel ZnMn₂O₄ cathode in Zn(CF₃SO₃)₂ electrolyte for rechargeable aqueous Zn-ion battery. *J. Am. Chem. Soc.* 2016; **138**: 12894-901.
36. Xia, C., Guo, J., and Lei, Y., *et.al.* Rechargeable aqueous zinc-ion battery based on porous framework zinc pyrovanadate intercalation cathode. *Adv. Mater.* 2018; **30**: 1705580.
37. Song, M., Tan, H., and Chao, D., *et.al.* Recent advances in zn-ion batteries. *Adv. Funct. Mater.* 2018; **28**: 1802564.

38. Wang, Z. Q., Winslow, R., and Madan, D., *et.al.* Development of MnO₂ cathode inks for flexographically printed rechargeable zinc-based battery. *J. Power Sources* 2014; **268**: 246-54.
39. Gaikwad, A. M., Whiting, G. L., and Steingart, D. A., *et.al.* Highly flexible, printed alkaline batteries based on mesh-embedded electrodes. *Adv. Mater.* 2011; **23**: 3251-55.
40. El-Kady, M. F. and Kaner, R. B. Scalable fabrication of high-power graphene micro-supercapacitors for flexible and on-chip energy storage. *Nat. Commun.* 2013; **4**: 9.
41. Pech, D., Brunet, M., and Durou, H., *et.al.* Ultrahigh-power micrometre-sized supercapacitors based on onion-like carbon. *Nat. Nanotechnol.* 2010; **5**: 651-54.
42. Chmiola, J., Largeot, C., and Taberna, P. L., *et.al.* Monolithic carbide-derived carbon films for micro-supercapacitors. *Science* 2010; **328**: 480-83.
43. Huang, J., Guo, Z., Ma, Y., *et.al.* Recent progress of rechargeable batteries using mild aqueous electrolytes. *Small Methods* 2018; **3**: 1800272.
44. Li, H., Liu, Z., and Liang, G., *et.al.* Waterproof and tailorable elastic rechargeable yarn zinc ion batteries by a cross-linked polyacrylamide electrolyte. *ACS Nano* 2018; **12**: 3140-48.
45. Sun, W., Wang, F., and Hou, S., *et.al.* Zn/MnO₂ battery chemistry with H⁺ and Zn²⁺ coinsertion. *J. Am. Chem. Soc.* 2017; **139**: 9775-78.

46. Wu, B., Zhang, G., and Yan, M., *et.al.* Graphene scroll-coated alpha-MnO₂ nanowires as high-performance cathode materials for aqueous zn-ion battery. *Small* 2018; **14**: 1703850.
47. Ding, J., Du, Z., and Gu, L., *et.al.* Ultrafast Zn²⁺ intercalation and deintercalation in vanadium dioxide. *Adv. Mater.* 2018; **30**: 1800762.
48. Konarov, A., Voronina, N., and Jo, J. H., *et.al.* Present and future perspective on electrode materials for rechargeable zinc-ion batteries. *ACS Energy Lett.* 2018; **3**: 2620-40.
49. Fu, Y., Wei, Q., and Zhang, G., *et.al.* High-performance reversible aqueous zn-ion battery based on porous MnO_x nanorods coated by MOF derived N-doped carbon. *Adv. Energy Mater.* 2018; **8**: 1801445.
50. Chao, D., Zhu, C., and Yang, P., *et.al.* Array of nanosheets render ultrafast and high-capacity Na-ion storage by tunable pseudocapacitance. *Nat. Commun.* 2016; **7**: 12122.
51. Chao, D. L., Liang, P., and Chen, Z., *et.al.* Pseudocapacitive na-ion storage boosts high rate and areal capacity of self-branched 2D layered metal chalcogenide nanoarrays. *ACS Nano* 2016; **10**: 10211-19.
52. El-Kady, M. F., Strong, V., and Dubin, S., *et.al.* Laser scribing of high-performance and flexible graphene-based electrochemical capacitors. *Science* 2012; **335**: 1326-30.

53. Liu, J., Guan, C., and Zhou, C., *et.al.* A flexible quasi-solid-state nickel–zinc battery with high energy and power densities based on 3D electrode design. *Adv. Mater.* 2016; **28**: 8732-39.
54. Zhao, T., Zhang, G., and Zhou, F., *et.al.* Toward tailorable Zn-ion textile batteries with high energy density and ultrafast capability: Building high-performance textile electrode in 3D hierarchical branched design. *Small* 2018; **14**: 1802320.

Figure Captions

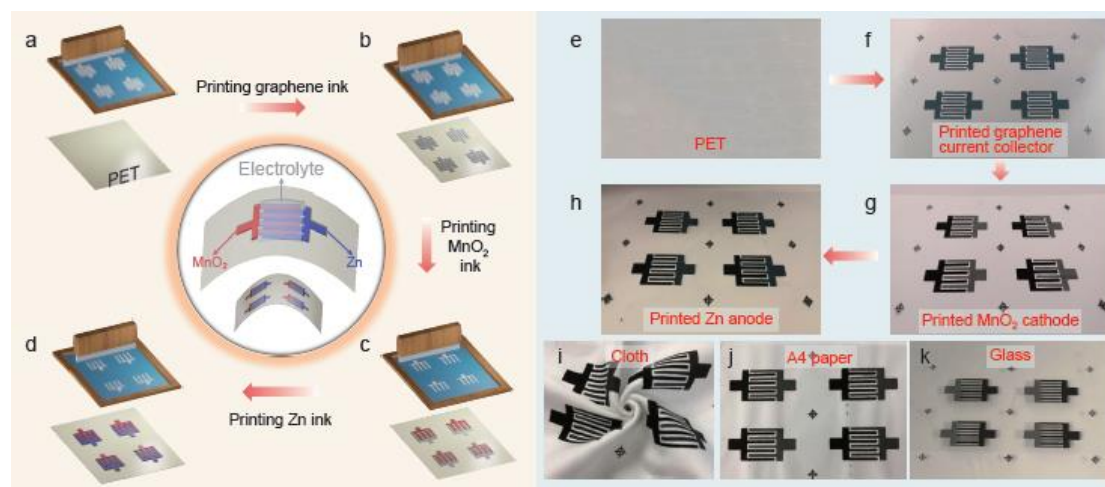


Figure 1. Fabrication of printed Zn//MnO₂ planar MBs. (a-d) Schematic of screen printing fabrication of printed Zn//MnO₂ MBs: (a) black PET substrate, (b) printed graphene current collectors, (c) printed MnO₂ cathode, (d) printed Zn anode. (e-h) Optical photographs showing the stepwise printing fabrication of Zn//MnO₂ MBs: (e) black PET substrate, (f) graphene current collectors, (g) printed MnO₂ cathode and (h) printed Zn anode on the interdigital graphene fingers. (i-k) Zn//MnO₂ MBs printed onto the different substrates, including (i) cloth, (j) A4 paper, and (k) glass.

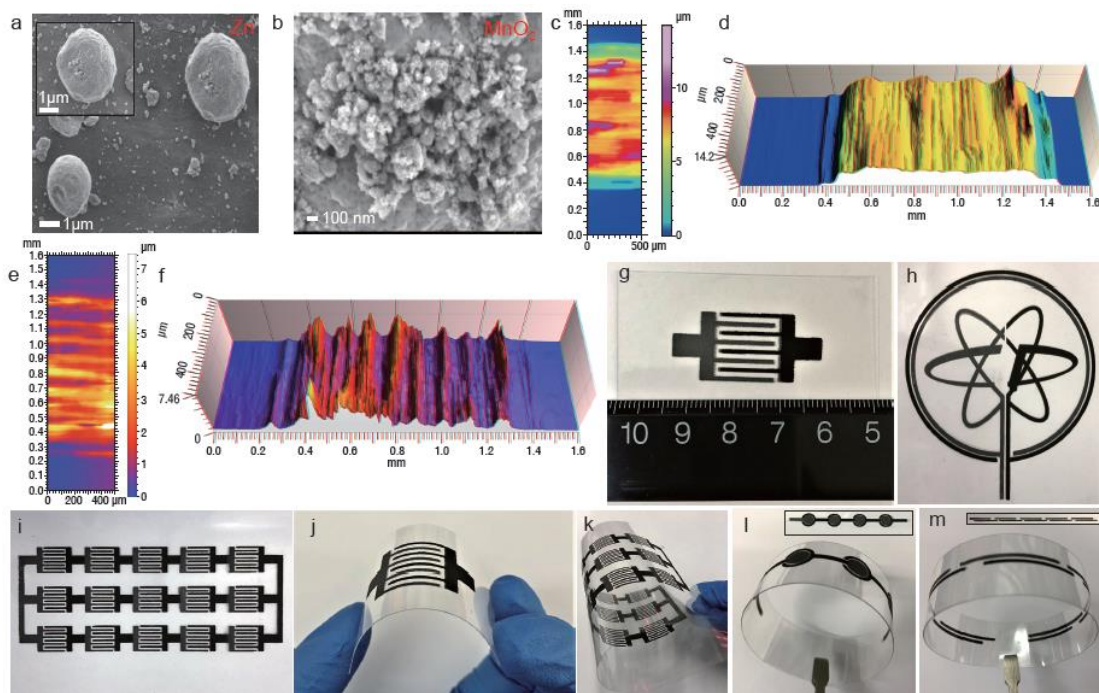


Figure 2. Characterization and shape diversity of printed Zn//MnO₂ planar MBs. (a, b) SEM images of (a) Zn anode and (b) MnO₂ cathode. (c) 2D pseudo-color view and (d) 3D view of MnO₂ microelectrode finger on PET substrate, showing the microelectrode thickness of ~9.8 μm. (e) 2D pseudo-color view and (f) 3D view of Zn microelectrode finger on PET substrate, showing the microelectrode thickness of 6.4 μm. (g-i) Photographs of flexible Zn//MnO₂ MBs with various shape diversity, such as (g) individual interdigital structure, (h) “DICP” logo based Zn//MnO₂ MBs, and (i) an energy storage pack of Zn//MnO₂ MBs connected in a tandem fashion of 5 series × 3 parallel. (j-m) Photographs of shape-designable Zn//MnO₂ MBs under different bending states, e.g., (j) an individual interdigital Zn//MnO₂ MBs, and (k) the tandem energy storage packs via self-connection of (g) interdigital Zn//MnO₂ MBs in 5 series × 3 parallel bended at 180°, (l) four concentric-circle-shape, and (m) five linear-shape Zn//MnO₂ MBs in series, under a flat and bending (180°) states.

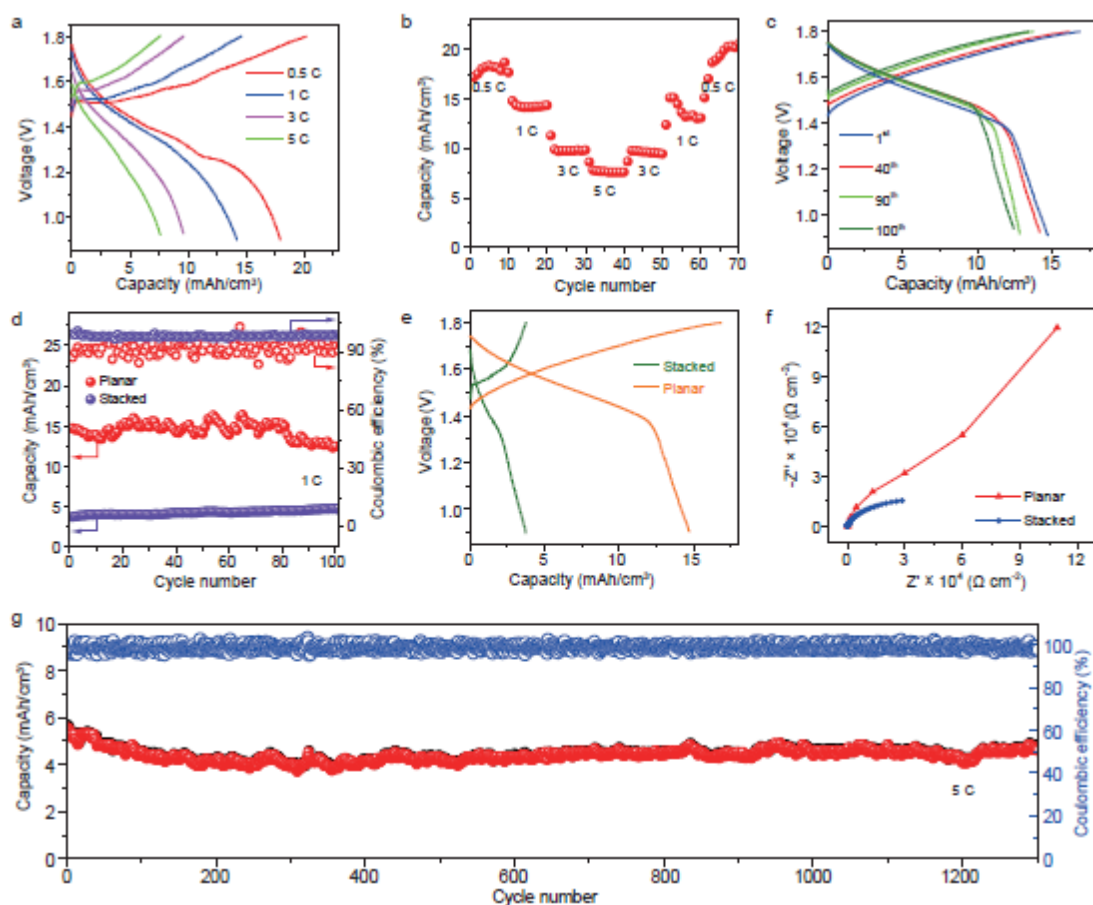


Figure 3. Electrochemical performance of printed Zn//MnO₂ planar MBs. (a) The GCD profiles, and (b) rate capability of Zn//MnO₂ MBs obtained from 0.5 C to 5 C. (c) The 1st, 40th, 90th, 100th GCD profiles, measured at a low rate of 1 C (15 mA/cm²). (d) Cycling stabilities of printed Zn//MnO₂ MBs with planar and sandwich-like stacked geometries, measured at 1 C rate. (e) The GCD profiles of the planar and stacked Zn//MnO₂ MBs. (f) EIS normalized to 1 of the planar and stacked Zn//MnO₂ MBs. (g) Long-term cycling stability of planar Zn//MnO₂ MBs over 1300 times at a high rate of 5 C.

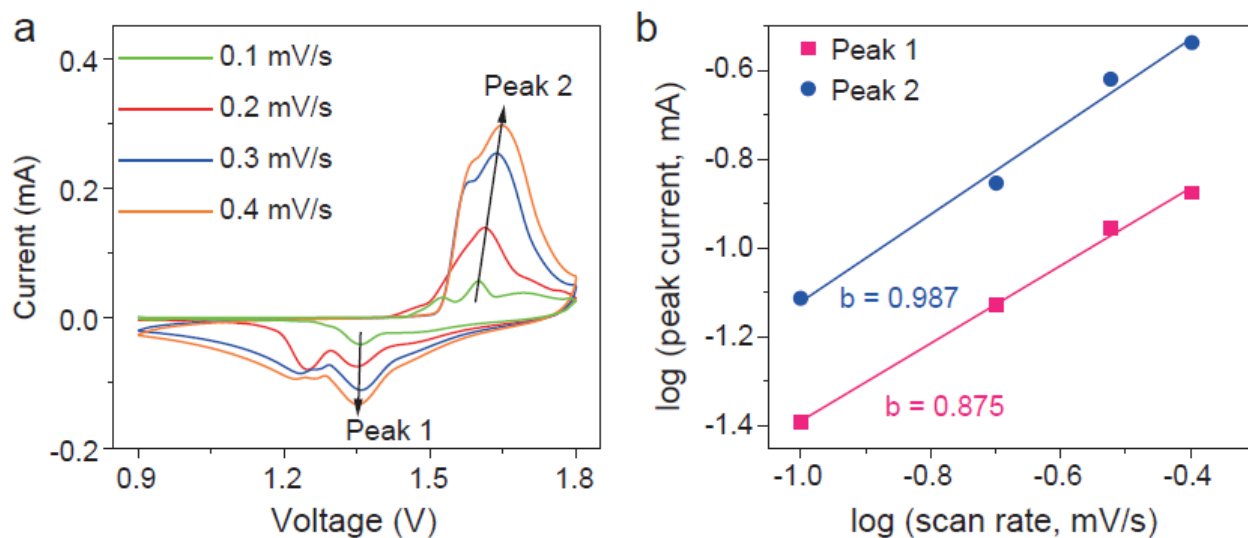


Figure 4. Kinetics analysis of ion intercalation of printed Zn/MnO₂ planar MBs. (a) CV curves of Zn/MnO₂ MBs obtained at various scan rates (v) from 0.1 to 0.4 mV/s. (b) The plots of $\log(i)$ versus $\log(v)$ curves of cathodic and anodic peaks.

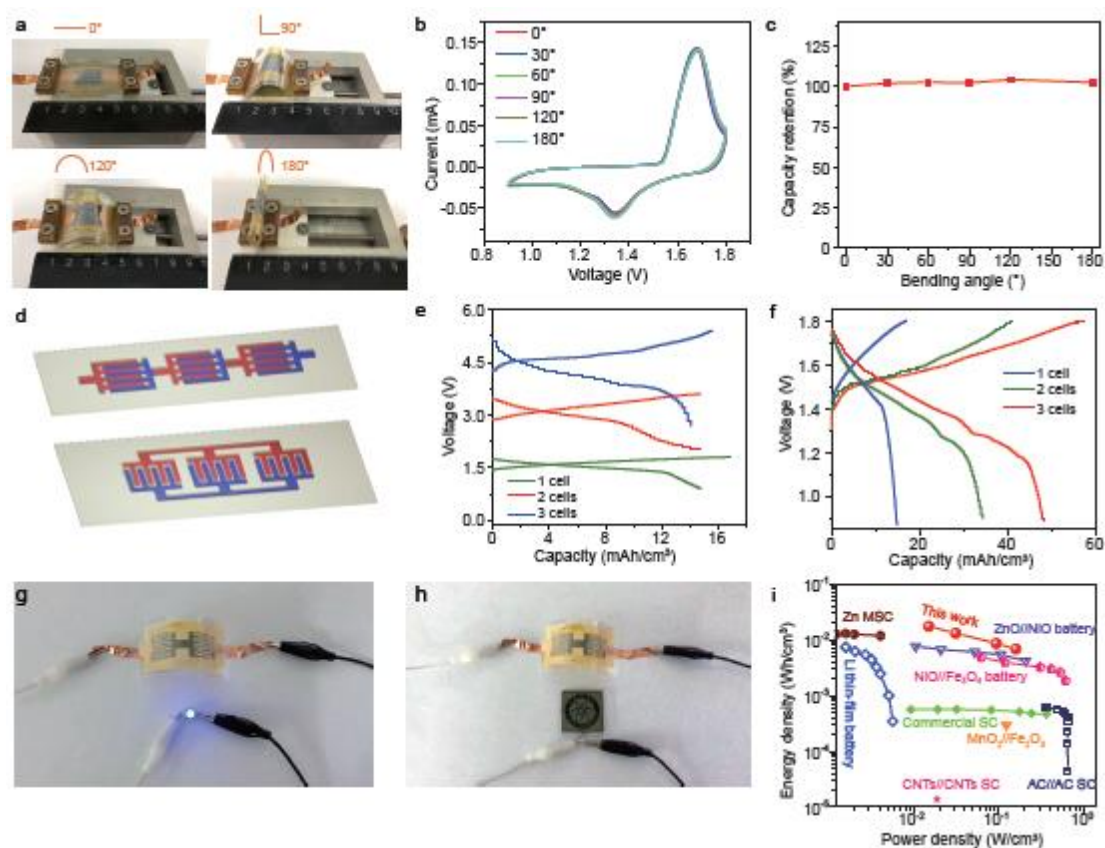


Figure 5. Exceptional flexibility and integration of Zn//MnO₂ planar MBs. (a) Photographs, (b) CV curves, and (c) capacity retention of Zn//MnO₂ MBs tested under different bending angles. (d) Schematic illustration of the integrated Zn//MnO₂ MBs connected three cells in series (up) and in parallel (bottom). (e, f) GCD profiles of the integrated Zn//MnO₂ MBs connected (e) in series and (f) in parallel from 1 to 3 cells. (g, h) Photographs of two serially-connected Zn//MnO₂ MBs, (g) lighting up a LED, and (h) to power a display of our institute “DICP” logo under the flexible state. (i) Ragone plot of Zn//MnO₂ MBs compared with other microscale energy-storage devices (AC: active carbon, CNTs: carbon nanotubes).